Int. J. Non-Linear Mechanics, Vol. 27, No. 2, pp. 279–291, 1992
Printed in Great Britain.

0020–7462/92 $5.00 + .00
Pergamon Press plc

EFFECT OF INITIAL TEMPERATURE ON THE INITIATION AND GROWTH OF SHEAR BANDS IN A PLAIN CARBON STEEL

C. H. KIM and R. C. BATRA*

Department of Mechanical and Aerospace Engineering and Engineering Mechanics, University of Missouri-Rolla, Rolla, MO 65401, U.S.A.

(*Received* 17 *July* 1990; *in revised form* 29 *October* 1990)

Abstract—We study thermomechanical deformations of a thermally softening viscoplastic block undergoing overall adiabatic simple shearing deformations. The dependence of the specific heat, thermal conductivity and shear modulus for the material of the block upon the temperature is accounted for. It is assumed that the block has a geometric defect in the sense that its thickness varies smoothly and is 5% less at the center as compared to that at the edges where essential mechanical boundary conditions are prescribed. It is found that with an increase in the initial temperature of the specimen the initiation of shear bands is delayed, and wider bands form.

1. INTRODUCTION

Adiabatic shear bands are narrow regions of intense plastic deformation that form during high strain-rate processes, such as shock loading, ballistic penetration, metal forming, and machining. As these bands generally precede material fracture, a knowledge of factors that inhibit or enhance their growth is essential to the production of durable materials and more efficient manufacturing processes. These bands form in both ferrous and non-ferrous alloys, and are called adiabatic because at high rates of deformation, there is not enough time for the heat to be conducted away from the bands.

In 1878, Tresca [1] observed hot lines during the forging of a platinum bar and stated that these were the lines of greatest development of heat. Subsequently, Massey [2] also observed these hot lines in 1921 during the hot forging of a metal and stated that "when diagonal 'slipping' takes place, there is great friction between particles and a considerable amount of heat is generated". These hot lines are now referred to as adiabatic shear bands. During the last decade there has been a surge of activity in understanding parameters that influence the initiation and growth of adiabatic shear bands.

Besides the experimental observations of Tresca and Massey, those reported by Zener and Hollomon [3], Moss [4], Costin *et al.* [5], Hartley *et al.* [6], Wulf [7], Marchand and Duffy [8] and Giovanola [9] have contributed enormously to our understanding of the initiation and growth of shear bands. Most of the analytical [10–18] and numerical [19–24] work aimed at understanding factors that enhance or inhibit the initiation and subsequent development of shear bands have involved analyzing overall simple shearing deformations of a viscoplastic block. Recently, there have been a few studies [25–34] of the phenomenon of shear banding in plane strain deformations of a viscoplastic block.

Based on their observations of the formation of shear bands in thin-walled HY-100 steel tubes, Marchand and Duffy [8] have proposed that the localization of deformation into narrow shear bands occurs in three stages. During stage one the body deforms homogeneously. Stage two begins when the shear stress attains its peak value. At this point, the softening caused by the heating of the material equals the hardening due to strain and strain rate. During stage two the body deforms non-homogeneously. The initiation of stage three is indicated by a precipitous drop in the shear stress at a point in the body and the simultaneous localization of the deformation into a narrow band. These three stages of the deformation have also been confirmed by numerical work [10, 19]. It is still unclear when stage three initiates. We note that the thin-walled tubes used by Marchand and Duffy had approximately 5% thickness variation along the axis of the tube.

Contributed by K. R. Rajagopal.
* Also Senior Research Investigator, Intelligent Systems Center.

The specific heat and the thermal conductivity of plain carbon steels depend rather strongly upon the temperature. Loosely speaking, the specific heat first increases with the rise in temperature until the phase transformation from pearlite to austenite occurs at which point the specific heat drops sharply and stays essentially constant with the further rise in the temperature. The shear modulus and the thermal conductivity decrease slowly with rise in the temperature. Since in the development of shear bands thermal softening caused by the heating of the material plays a key role, it is imperative that we account for the temperature dependence of the specific heat and thermal conductivity. For the same reason the initial temperature of the specimen will influence significantly the average strain when a shear band initiates and its subsequent development. Wang *et al.* [35] tested titanium alloy TB2 (Ti-8 Cr-5MO-5V-3Al) specimens in compression at various environmental temperatures and concluded that the susceptibility to adiabatic shearing increased at lower environmental temperatures. The computed results presented herein agree with this observation. Also the band width increases with an increase in the initial temperature of the specimen.

2. FORMULATION OF THE PROBLEM

We study dynamical thermomechanical deformations of an isotropic and thermally softening viscoplastic block undergoing overall adiabatic simple shearing deformations. We choose a fixed set of rectangular cartesian coordinate axes with origin at the lower surface of the block and the direction of shearing along the x-axis. The governing equations are:

$$\rho\omega\dot{v} = (\omega s)_{,y}, \quad 0 < y < H \tag{2.1}$$

$$\rho c(\theta)\omega\dot{\theta} = [\omega k(\theta)\theta_{,y}]_{,y} + \omega s\dot{\gamma}_p, \quad 0 < y < H \tag{2.2}$$

$$\dot{\gamma} = v_{,y} = \dot{\gamma}_e + \dot{\gamma}_p \tag{2.3}$$

$$\dot{s} = \mu(\theta)\dot{\gamma}_e \tag{2.4}$$

$$\dot{\gamma}_p = D_0 \exp\left[-\frac{1}{2}\left(\frac{Z^2}{3s^2}\right)^n\right], \qquad n = \frac{a}{\theta} + b \tag{2.5}$$

$$Z = Z_1 - (Z_1 - Z_0)\exp(-mW_p) \tag{2.6}$$

$$\dot{W}_p = s\dot{\gamma}_p. \tag{2.7}$$

Equation (2.1) expresses the balance of linear momentum and equation (2.2) the balance of internal energy. Equation (2.4) is Hooke's law written in the rate form, and equation (2.5) is the Bodner–Partom law [36] that relates the plastic strain rate to the shear stress s, the temperature θ in degrees Kelvin, and the deformation history through W_p that equals the density of the plastic work done at a material point. In equations (2.1)–(2.7), ρ is the mass density, v the velocity of a material particle in the direction of shearing, ω the thickness of the block, c the specific heat, k the thermal conductivity, $\dot{\gamma}_p$ the plastic strain rate, μ the shear modulus, $\dot{\gamma}_e$ the elastic strain rate, a comma followed by y signifies partial differentiation with respect to y, and a superimposed dot indicates the material time derivative. We note that equations (2.4) and (2.5) are constitutive hypotheses and in writing equation (2.2) we have implicitly assumed that Fourier's law of heat conduction holds. In equations (2.5)–(2.7), D_0 is the limiting value of the plastic strain rate and is generally set equal to $10^8\ s^{-1}$, and parameters a, Z_1, Z_0, m and b characterize the plastic response of the material. We note that there is no loading or yield surface assumed herein. Also changes in the mass density due to thermal expansion of the body have been neglected and, accordingly, the mass density is regarded as a constant.

In terms of non-dimensional variables, indicated below by a superimposed bar,

$$\bar{y} = y/H, \quad \bar{t} = v_0 t/H, \quad \bar{\omega} = \omega/H, \quad \bar{\theta} = \theta/\theta_0, \quad \theta_0 = \sigma_0/\rho c_R$$
$$\bar{s} = s/\sigma_0, \quad \bar{Z} = Z/\sigma_0, \quad \bar{Z}_1 = Z_1/\sigma_0, \quad \bar{Z}_0 = Z_0/\sigma_0$$
$$\bar{D}_0 = D_0 H/v_0, \quad \dot{\bar{\gamma}}_p = \dot{\gamma}_p H/v_0, \quad \dot{\bar{W}}_p = \dot{W}_p H/(\sigma_0 v_0) \tag{2.8}$$
$$\alpha = \rho v_0^2/\sigma_0, \quad \beta = k_R/(\rho v_0 c_R H), \quad \bar{c} = c(\theta)/c_R, \quad \bar{k} = k/k_R, \quad \bar{\mu} = \mu/\mu_R$$
$$k_R = k(\theta_R), \quad c_R = c(\theta_R), \quad \mu_R = \mu(\theta_R), \quad \bar{m} = m\sigma_0, \quad \theta_R = 300\,^{\circ}\mathrm{K}$$

equations (2.1) and (2.2) become

$$\alpha\omega\dot{v} = (\omega s)_{,y}, \qquad 0 < y < 1 \tag{2.9}$$

$$c\omega\dot{\theta} = \beta(\omega k\theta_{,y})_{,y} + \omega\dot{W}_p, \qquad 0 < y < 1 \tag{2.10}$$

where we have dropped the superimposed bars. The form of equations (2.3)–(2.7) remains unchanged except that the variables used are non-dimensional. In equation (2.8), v_0 is the final value of the speed imposed on the top surface of the block, σ_0 is the yield stress in a quasi-static simple shearing test, and θ_R is the reference temperature. The value of the non-dimensional parameter α in equation (2.9) signifies the effect of inertia forces compared to the flow stress of the material. For initial and boundary conditions we take

$$\begin{gathered} v(y,0) = 0, \qquad s(y,0) = 0, \qquad \theta(y,0) = \theta_a, \qquad W_p(y,0) = 0 \\ v(1,t) = \begin{cases} t/0.01, & 0 \leqslant t \leqslant 0.01 \\ 1, & t \geqslant 0.01 \end{cases} \\ \theta_{,y}(0,t) = 0, \qquad \theta_{,y}(1,t) = 0. \end{gathered} \tag{2.11}$$

That is, the block is initially at rest, is stress free and is at a uniform temperature θ_a. The lower and upper surfaces of the block are assumed to be perfectly insulated, the lower surface is kept fixed while on the top surface, the prescribed shearing speed increases from 0 to 1.0 in a non-dimensional time of 0.01. For the thickness variation, we take

$$\omega(y) = \omega_0\left[1 + \frac{\delta}{2}\sin\left(\frac{1}{2} + 2y\right)\pi\right]. \tag{2.12}$$

Thus the block is thinnest at the center ($y = \frac{1}{2}$) and thickest at the bounding surfaces, $y = 0, 1$.

The coupled partial differential equations (2.9), (2.10) and those obtained from (2.3)–(2.7) are highly non-linear. An approximate solution of these equations under the side conditions (2.11) with ω given by equation (2.12) is found numerically. The governing equations are first reduced to a set of coupled ordinary non-linear differential equations by using the Galerkin approximation. These equations are then integrated with respect to time t by using the Gear method [37]. For this purpose the subroutine LSODE included in the package ODEPACK developed by Hindmarsh [38] has been used. The details of the method are given in Batra and Kim [20].

3. RESULTS

In order to compute results, we assigned the following values to various variables.

$$\begin{gathered} H = 2.5\text{ mm}, \qquad v_0 = 2.5\text{ m/s}, \qquad \omega_0 = 0.38\text{mm}, \qquad \delta = 0.05, \\ \sigma_0 = 405\text{ MPa}, \qquad \rho = 7850\text{ kg/m}^3, \qquad c_R = 426\text{ J/kg °K}, \qquad k_R = 63.6\text{ W/m °K}, \\ Z_1 = 3.778, \qquad Z_0 = 3.185, \qquad m = 2.5, \qquad \mu_R = 78.3\text{ GPa} \\ \theta_R = 300\text{ °K}, \qquad a = \theta_{\text{melt}} = 1800\text{ °K}, \qquad D_0 = 3300, \qquad b = 0. \end{gathered} \tag{3.1}$$

These values are for a plain carbon steel, and are such that for $\theta_a = 300$ °K and $\dot{\gamma}_{\text{avg}} = 3300\text{ s}^{-1}$, the average shear stress–average shear strain curve obtained in the numerical simulation of the simple shear test on a block of uniform thickness mimics well the stress–strain curve given by Marchand and Duffy [8] for the HY-100 steel. By comparing predictions from five constitutive relations, namely, the Litonski law, Batra–Wright dipolar theory, power law, Bodner–Partom law, and the Johnson–Cook law, with the experimental observations of Marchand and Duffy [8], Batra and Kim [21] concluded that the Wright–Batra dipolar theory and the Bodner–Partom law predict most aspects of the localization process better than the other three constitutive relations. However, the range of validity of the Bodner–Partom law with material variables assigned values in equation (3.1) is uncertain because of the lack of availability of the experimental data. The dependence of the thermal conductivity, specific heat and shear modulus upon temperature, taken from [39], is illustrated in Fig. 1. The homologous temperature for a material point is defined as

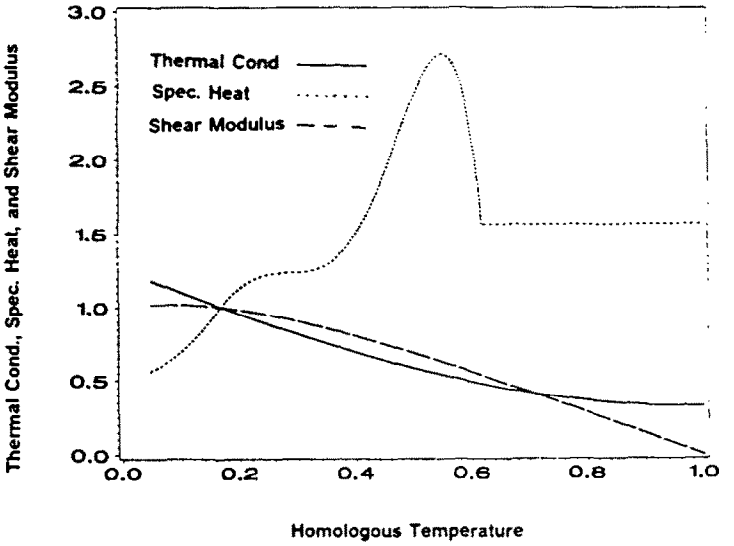

Fig. 1. Dependence of the thermal conductivity, specific heat and shear modulus for the material of the block upon the temperature.

the ratio of its absolute temperature to the melting temperature θ_{melt} of the material. The sharp drop in the value of the specific heat at a homologous temperature of 0.54 corresponds to the phase transformation in steel. For assigned values of H and v_0, the nominal strain rate equals 1000 s^{-1}. We have assumed that the block has a geometric defect and its thickness at the center is 5% less than that at the edges. The finite-element mesh used is such that a large number of nodes are concentrated near the center, where the shear band is expected to develop. The y-coordinate of the nth node is given by

$$y_n = 4\left(\frac{n-1}{100} - 0.5\right)^3 + \frac{1}{2}, \quad n = 1, 2, 3, \ldots, 101. \tag{3.2}$$

We have carried out the investigation for six different values of the initial temperature, namely, $\theta_a = 83$, 200, 300, 343, 407 and 523 °K. In the results presented below, curves corresponding to different values of θ_a are distinguished as follows.

Curve type	θ_a (°K)
(——————)	523
(- - - - - - - -)	407
(—— —— —— —— ——)	343
(——— - ———)	300
(—— - - ——)	200
(—— — — ——)	83

Figure 2 depicts the evolution of the average shear stress s_a, defined as

$$s_a = \int_0^1 s\,dy$$

and the homologous temperature at the center of the specimen as it is deformed. As expected, with an increase in the initial temperature θ_a of the specimen, the maximum value s_{max} of the average shear stress decreases. Also with an increase in θ_a, the average strain at which s_{max} occurs, increases and the stress drop becomes more gradual. We should note that at $\gamma_{avg} = 1000\ s^{-1}$, inertia forces do not play an important role and the shear stress depends upon y because of the dependence of ω upon y. At about the instant the shear stress begins to drop, the homologous temperature at the center of the specimen increases and the rate of temperature rise approximately equals the rate of stress drop. This becomes more evident from the plots of the homologous temperature θ_c at the center of the specimen vs s_a/s_{max}

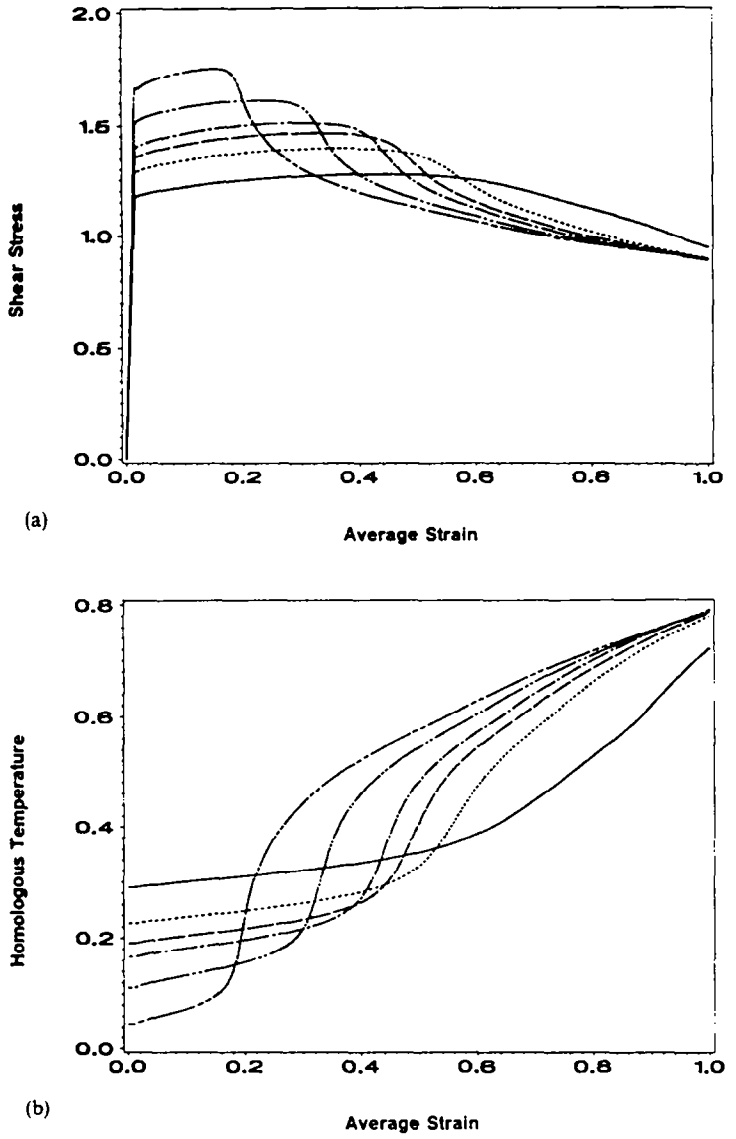

Fig. 2. (a) Average shear stress vs the average shear strain for six different values of the initial temperature of the specimen. (b) Homologous temperature at the center of the specimen vs the average shear strain.

given in Fig. 3a. Note that s_a/s_{max} and the average strain correspond to different time scales along the abscissa. Since the shear stress drops rapidly [19, 20] during the time a shear band develops, s_a/s_{max} represents expanded time scale. During the time interval when $0.75 \leqslant s_a/s_{max} \leqslant 0.95$, these plots are essentially parallel straight lines. For $s_a/s_{max} \leqslant 0.75$, these curves become convex upwards and the deviation from the straight-line behavior decreases with an increase in the initial temperature of the specimen. In Fig. 3b, we have plotted the homologous temperature at the specimen center vs the normalized average strain. Since the average strain γ_s at which s_{max} occurs depends upon the initial temperature of the specimen, and the sharp rise in the temperature occurs after the shear stress begins to drop, we have normalized the average strain with respect to γ_s. The shapes of these curves, except that for $\theta_a = 523\,°K$, change from convex upwards to convex downwards at $\gamma/\gamma_s \simeq 1.4$. The curvature of the convex downwards part of the curve decreases as θ_a increases. The curve for $\theta_a = 523\,°K$ remains convex upwards.

The distribution of the plastic strain within the specimen at three different values of s_a/s_{max} is plotted in Fig. 4. One can conclude from these plots that a narrow region near the center of the specimen undergoes considerably more severe deformations as compared to

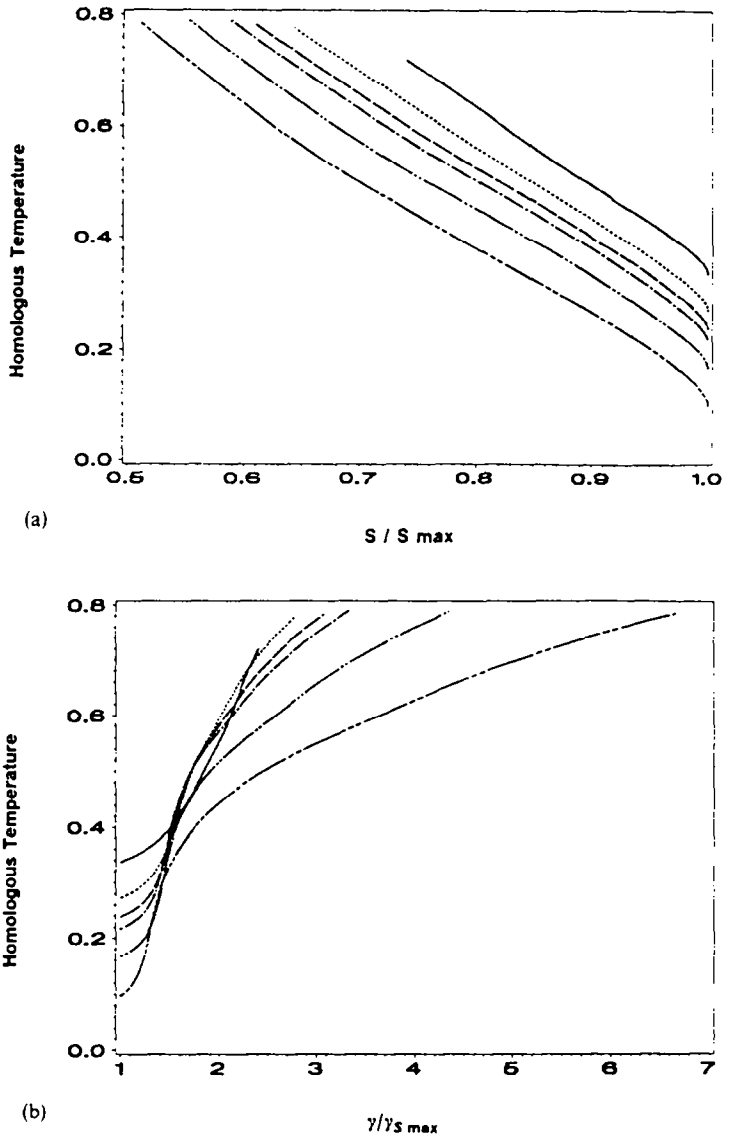

Fig. 3. Evolution of the temperature at the center of the specimen: (a) homologous temperature at the center vs s_a/s_{max}, (b) homologous temperature at the center of the specimen vs γ_{avg}/γ_s. Here γ_s equals the value of γ_{avg} when the average shear stress attains its maximum value.

those experienced by the material near the outer edges. For a given value of s_a/s_{max}, the width of this severely deforming region increases with an increase in the value of θ_a. The width of this severely deforming region continues to decrease with the drop in the value of the shear stress at the specimen center. Another way to study the localization of the deformation is to observe at different instants the deformed position of an initially straight-line. We recall that Marchand and Duffy [8] use this technique to find the plastic strain at a point. In Fig. 5, we have plotted the deformed positions of an initially straight-line at $s_a/s_{max} = 1.0$, 0.95, 0.85 and 0.75. For each value of θ_a considered, the deformation has become non-homogeneous by the time the average shear stress s_a attains its peak value. As θ_a increases, the width of the central region that has undergone more deformations as compared to the deformations of the outer region increases. At $s_a/s_{max} = 0.95$, the localization of the deformation near the center of the specimen becomes evident at $\theta_a = 83\,^{\circ}K$ but is less transparent for other values of θ_a considered. However, the plots in Fig. 4 indicate that the deformation at other values of θ_a has also begun to localize near the center of the block when $s_a/s_{max} = 0.95$. At $s_a/s_{max} = 0.85$, the deformation has clearly localized near the center of the specimen. The width of this severely deforming region has narrowed down significantly by the time $s_a(t) = 0.75\, s_{max}$ and one may say that a shear band has fully developed.

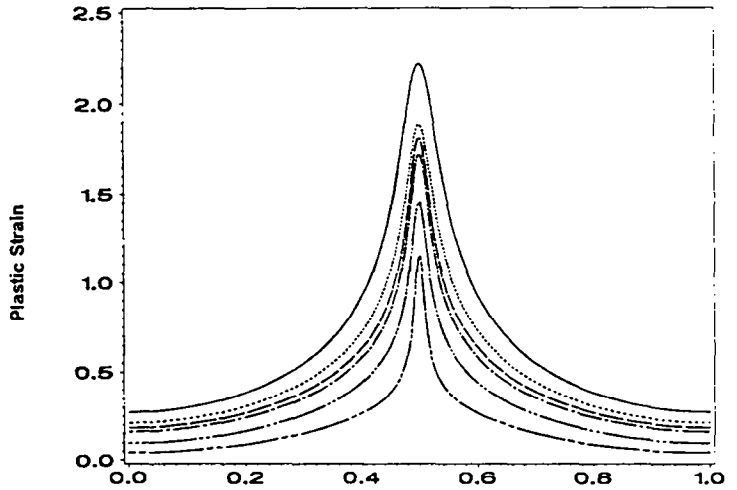

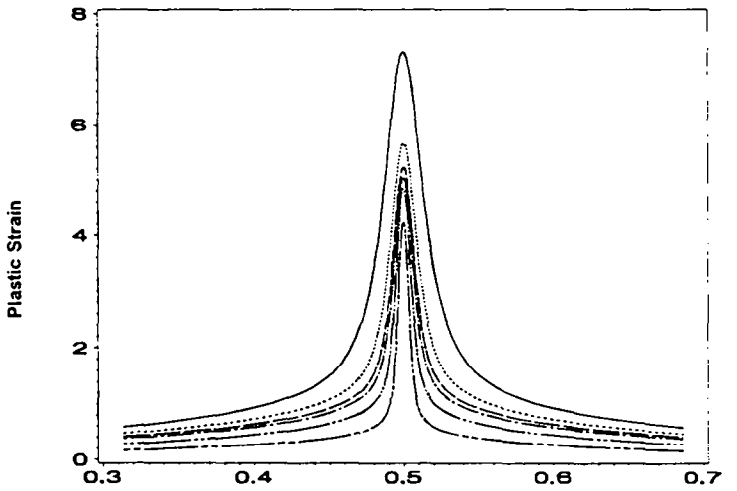

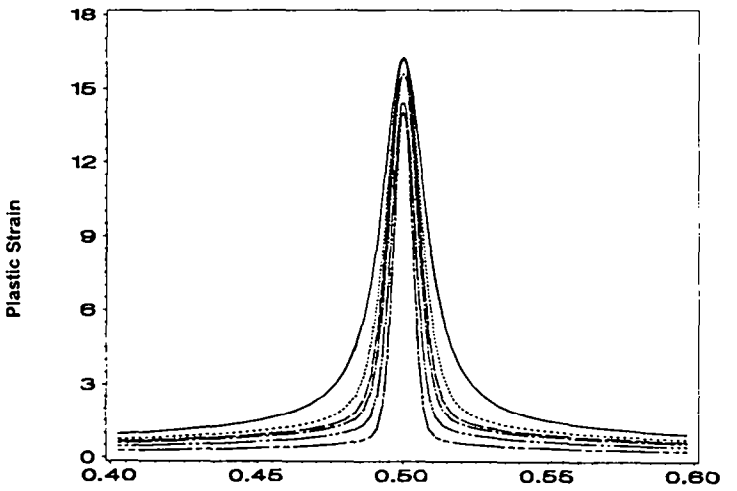

Fig. 4. Distribution of the plastic strain within the specimen at (a) $s_a/s_{max} = 0.95$, (b) $s_a/s_{max} = 0.85$, (c) $s_a/s_{max} = 0.75$.

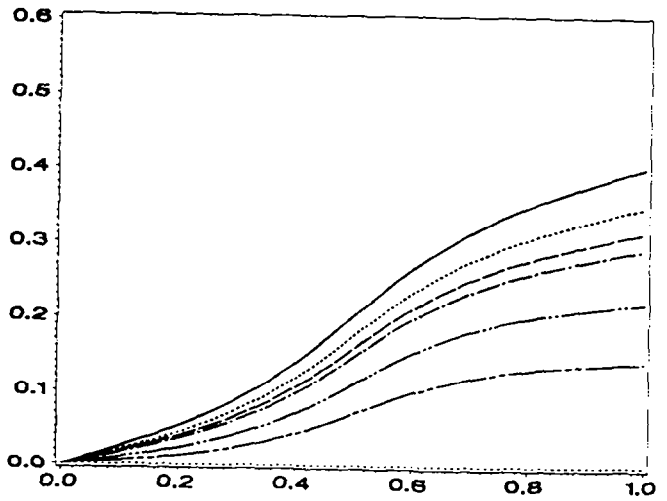

(a) Y - coordinate (S / S max = 1.00)

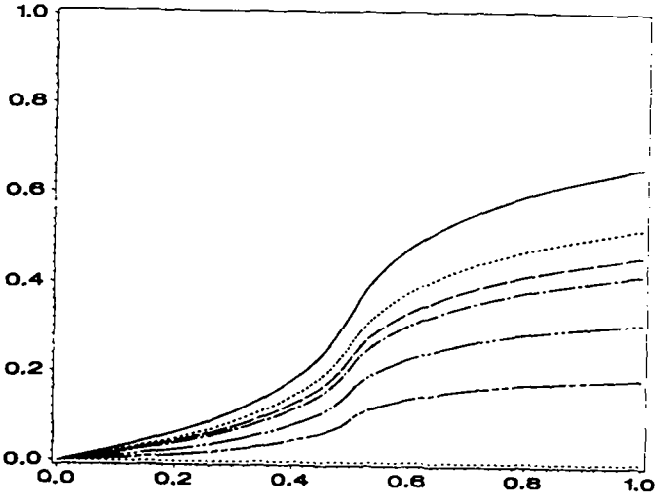

(b) Y - coordinate (S / S max = 0.95)

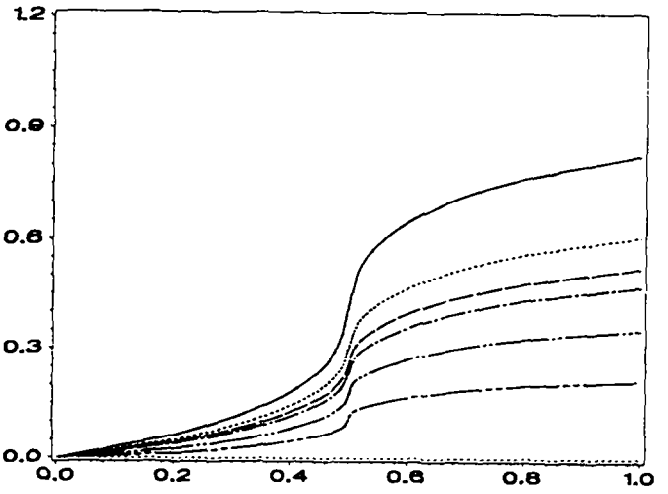

(c) Y - coordinate (S / S max = 0.85)

Fig. 5. (a)–(c).

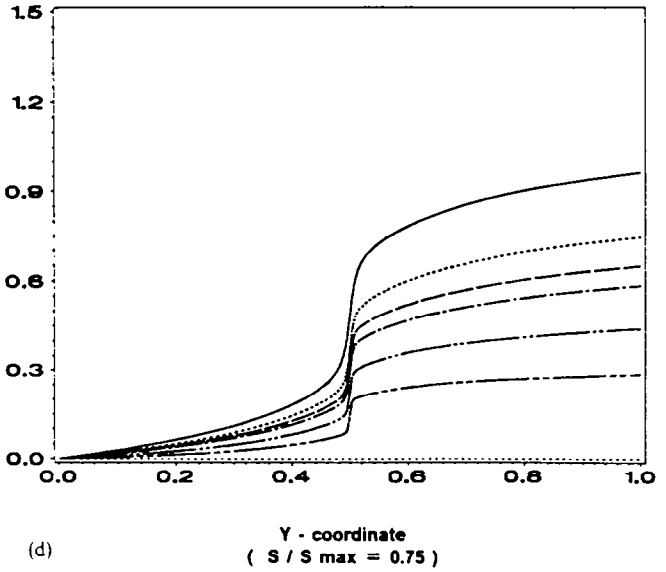

Fig. 5. Deformed shapes of an initial straight line at (a) $s_a/s_{max} = 1.0$, (b) $s_a/s_{max} = 0.95$, (c) $s_a/s_{max} = 0.85$, (d) $s_a/s_{max} = 0.75$. The ordinate equals the displacement of a point in the direction of shearing.

The deformed configurations of the initially straight-line vividly reveal that the shear strain γ_{loc} at the band center is very high. Figures 6a and 6b give the plots of γ_{loc} vs γ_{avg} and $(\gamma_{loc}/\gamma_{avg})$ vs s_a/s_{max}. The value of γ_{avg} when γ_{loc} begins to increase rapidly equals the nominal strain γ_i when a shear band initiates. Thus the value of γ_i increases noticeably with an increase in the value of θ_a. Also at higher values of θ_a, γ_{loc} increases slowly with γ_{avg} in the beginning implying thereby that the rate of development of a shear band decreases with an increase in the value of the initial temperature of the specimen. Once a shear band has fully formed, then γ_{loc} increases essentially linearly with γ_{avg} and the slopes of the nearly straight-line portions of the curves γ_{loc} vs γ_{avg} are independent of θ_a. The quantity $\gamma_{loc}/\gamma_{avg}$ which equals the ratio of the shear strain at the band center to the average strain in the specimen may be interpreted as the localization ratio. The plots in Fig. 6b indicate that for a given value of s_a/s_{max}, the localization ratio increases with a decrease in the value of θ_a. Thus when the shear stress at the band center has dropped to, say, 80% of s_{max}, more severe deformations have occurred at the band center if θ_a is less as compared to those for higher values of θ_a.

We now explore the dependence of the band width upon the initial temperature θ_a of the specimen. Marchand and Duffy [8] define the band width as the width of the region over which plastic strain stays constant and equals the maximum strain attained at any point in the specimen. This definition would give the band width as zero in the numerical work. Therefore, we define the band width as the width of the region surrounding the specimen center where the plastic strain is at least equal to 0.95 γ_{max}; γ_{max} equals the maximum plastic strain in the specimen. It is clear from the plastic strain distribution plotted in Fig. 4 that the band width depends upon s_a/s_{max}. The dependence of the band width upon s_a/s_{max} for different values of θ_a is shown in Fig. 7. We add that the finite-element mesh used had 20 elements within 5 μm wide region surrounding the specimen center. For each value of θ_a, the band width decreases with a drop in the value of the shear stress at the band center. For a given value of s_a/s_{max}, wider bands form at higher values of θ_a. As the shear stress drops below $s_a/s_{max} = 0.7$, the band width tends to stabilize. If all other material parameters are kept fixed, Batra and Kim [40] found that the band width increases with an increase in the value of the thermal conductivity. Figure 3a reveals that at $s_a/s_{max} = 0.75$, the homologous temperature at the specimen center is higher for larger values of θ_a. Hence, the thermal conductivity will be lower, and the band width should be smaller. But we get wider bands, because here the specific heat is also taken to vary with the temperature, and the initial specimen temperature is higher. In Fig. 8 we have plotted the dependence of various

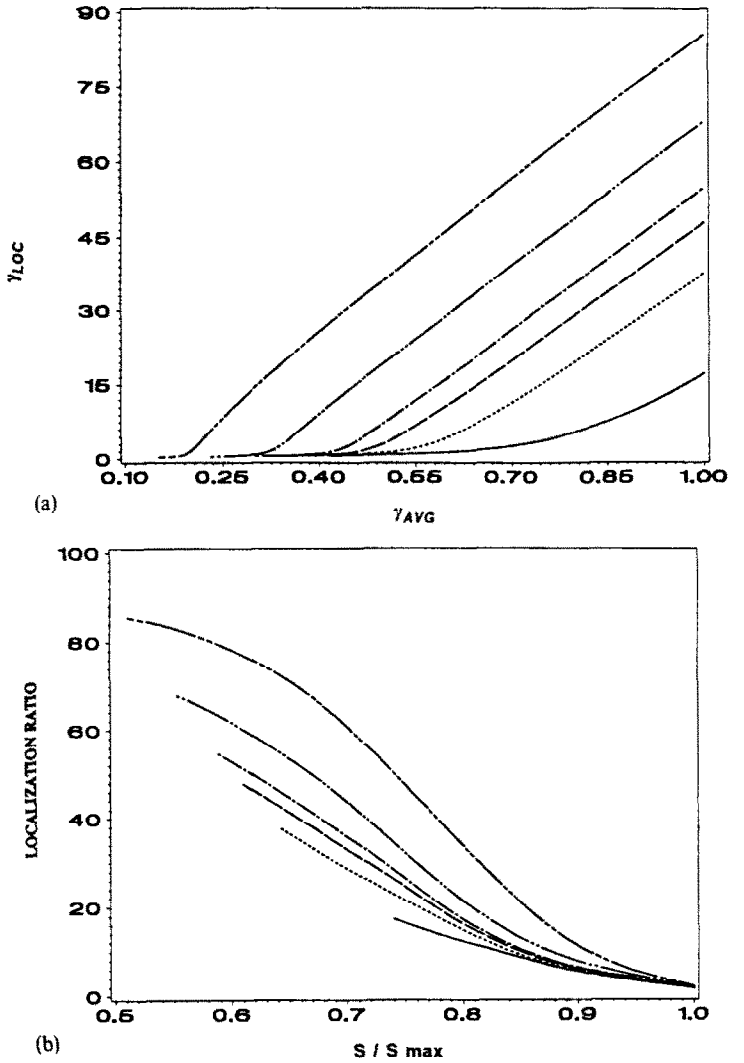

Fig. 6. (a) The shear strain γ_{loc} at the band center vs the nominal strain γ_{avg}. (b) The localization ratio $(\gamma_{loc}/\gamma_{avg})$ vs s_a/s_{max}.

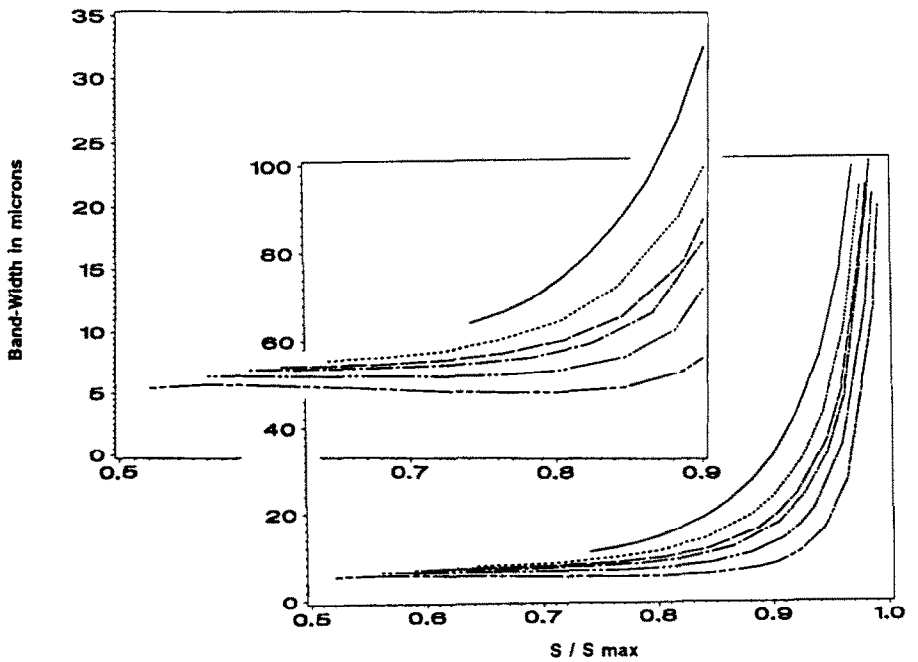

Fig. 7. Dependence of the band width upon s_a/s_{max}.

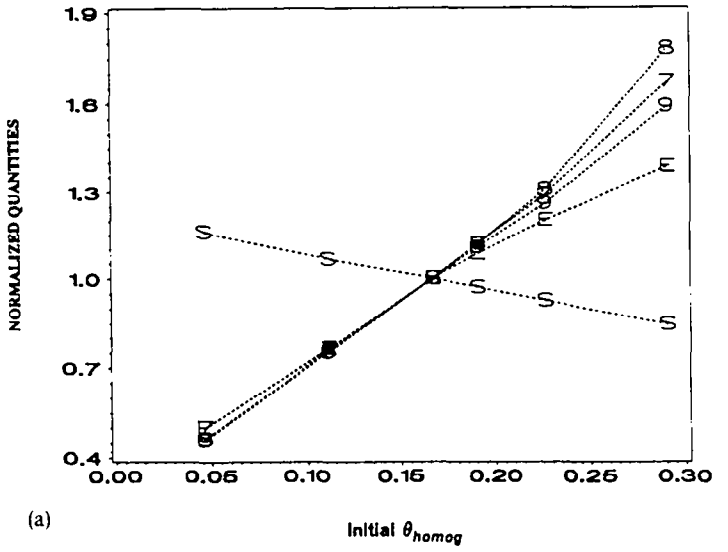

(a)

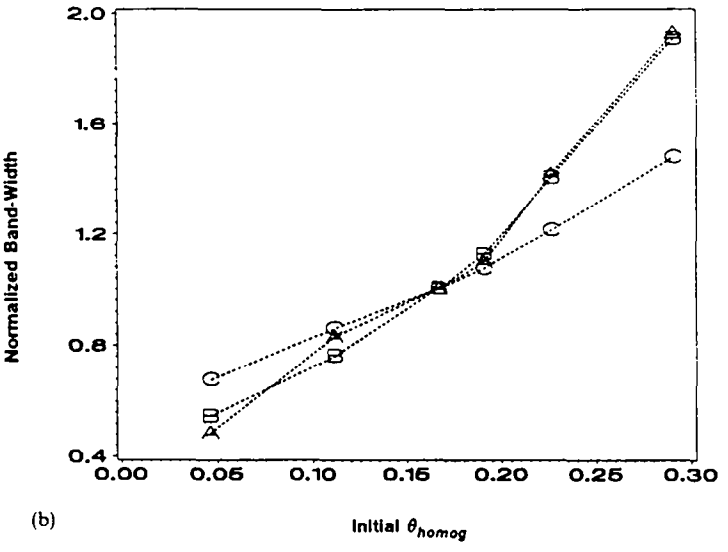

(b)

Fig. 8. (a) Dependence of normalized quantities upon θ_a. The quantities are normalized with respect to their values when the initial temperature of the specimen equals the room temperature. S = normalized s_{max}, E = normalized γ_{avg} when $s = s_{max}$, 9 = normalized γ_{avg} when $s_a = 0.95 s_{max}$, 8 = normalized γ_{avg} when $s_a = 0.85 s_{max}$, 7 = normalized γ_{avg} when $s_a = 0.75 s_{max}$. (b) Dependence of the band width, normalized with respect to its value when the initial temperature of the specimen equals the room temperature, upon θ_a. (A) $s_a/s_{max} = 0.95$, (B) $s_a/s_{max} = 0.85$, (C) $s_a/s_{max} = 0.75$.

normalized quantities upon θ_a. A quantity is normalized with respect to its value at the room temperature, taken to equal 300 °K. Even though the dependence of the shear stress upon temperature θ in the Bodner–Partom law is quite complicated, the value of normalized s_{max} decreases linearly with the rise in the initial temperature θ_a of the specimen. The value of the normalized γ_{avg} when the shear stress attains its maximum value increases first linearly with θ_a until $\theta_a = 0.18\theta_{melt}$ and subsequently this rate of increase slows down with an increase in the value of θ_a. However, the values of the normalized nominal strain when s_a/s_{max} equal 0.95, 0.85 and 0.75 first increase linearly with θ_a until $\theta_a = 0.18\theta_{melt}$, subsequently this rate of increase picks up with an increase in the value of θ_a. Note that $0.18\theta_{melt}$ equals the room temperature. The normalized band width increases with θ_a irrespective of the value of s_a/s_{max} when the band width is computed.

The aforementioned computed results can be explained as follows. For the same amount of plastic work done, because of the smaller value of the specific heat at lower temperatures, the temperature rise at lower values of θ_a is more than that at higher values of θ_a. Recall that

the thermal conductivity and the shear modulus do not depend upon the temperature as strongly as the specific heat does. The higher temperature rise at low values of θ_a softens the material more, and consequently the shear stress attains its peak value at lower values of the average strain. Because of the smaller thickness at the center of the specimen, the shear stress there is higher as compared to that at the edges of the specimen. The resulting greater value of W_p at the center of the specimen results in higher values of θ there. At low values of the initial temperature θ_a of the specimen, the temperature gradient near the center of the specimen is steeper than what it is at higher values of θ_a. Thus shear bands form more quickly at the center and are narrower than those at lower values of θ_a.

4. CONCLUSIONS

We have studied the effect of the initial specimen temperature upon the initiation and growth of shear bands in a viscoplastic body undergoing overall adiabatic simple shearing deformations. We have accounted for the dependence of the specific heat, thermal conductivity and the shear modulus upon the temperature and have solved numerically the coupled non-linear governing equations. It is found that the average strain at which shear bands form and the band width decrease with a decrease in the value of the initial temperature of the specimen. This has important implications in practical applications in that at higher initial temperatures of the specimen, larger changes of shape can be accommodated without damaging the workpiece due to the occurrence of shear bands.

Acknowledgements—This work was supported by the U.S. National Science Foundation Grant MSM 8715952 and the U.S. Army Research Office Contract DAAL03-88-K-0184 to the University of Missouri-Rolla. Some of the computations were performed on the NSF-sponsored supercomputer center in Ithaca, NY.

REFERENCES

1. H. Tresca, On further application of the flow of solids. *Proc. Inst. Mech. Engng* **30**, 301 (1878).
2. H. F. Massey, The flow of metal during forging. *Proc. Manchester Assoc. Engrs*, pp. 21–26 (1921). Reprinted by the National Machinery Co., Tiffon, OH (1946).
3. C. Zener and J. H. Hollomon, Effect of strain rate on plastic flow of steel. *J. appl. Phys.* **14**, 22 (1944).
4. G. L. Moss, Shear strain, strain rate and temperature changes in an adiabatic shear band, in *Shock Waves and High Strain Rate Phenomenon in Metals* (Edited by M. A. Meyer and L. E. Murr), pp. 299–312. Plenum Press, New York (1981).
5. L. S. Costin, E. E. Crisman, R. H. Hawley and J. Duffy, On the localization of plastic flow in mild steel tubes under dynamic torsional loading. *Int. Phys. Conf. Ser.* **47**, 90 (1979).
6. K. A. Hartley, J. Duffy and R. H. Hawley, Measurement of the temperature profile during shear band formation in steels deforming at high strain rates. *J. Mech. Phys. Solids* **35**, 283 (1987).
7. G. L. Wulf, The high strain rate compression of 7039 aluminum. *Int. J. Mech.* **20**, 609 (1978).
8. A. Marchand and J. Duffy, An experimental study of the formation process of adiabatic shear bands in a structural steel. *J. Mech. Phys. Solids* **36**, 251 (1988).
9. J. H. Giovanola, Adiabatic shear banding under pure shear loading. Part I: Direct observation of strain localization and energy dissipation measurements. *Mechs. Mater.* **7**, 59 (1988).
10. A. Molinari and R. J. Clifton, Analytic characterization of shear localization in thermoviscoplastic materials. *ASME J. appl. Mech.* **54**, 806 (1987).
11. R. F. Recht, Catastrophic thermoplastic shear. *ASME J. appl. Mech.* **31**, 189 (1964).
12. M. R. Staker, The relation between adiabatic shear instability strain and material properties. *Acta Metal.* **29**, 683 (1981).
13. T. J. Burns, Approximate linear stability analysis of a model of adiabatic shear band formation. *Quart. appl. Math.* **43**, 65 (1985).
14. R. J. Clifton, Adiabatic shear banding, in *Material Response to Ultra High Loading Rates*, Chapter 8, NRC National Material Advisory Board (U.S.) Report NMAB-356, pp. 129–142 (1980).
15. B. D. Coleman and M. L. Hodgdon, On shear bands in ductile materials. *Arch. Rat. Mech. Anal.* **90**, 219 (1985).
16. T. W. Wright, Steady shearing in a viscoplastic solid. *J. Mech. Phys. Solids* **35**, 269 (1987).
17. L. Anand, K. H. Kim and T. G. Shawki, Onset of shear localization in viscoplastic solids. *J. Mech. Phys. Solids* **35**, (1987).
18. Y. L. Bai, A Criterion for thermoplastic shear instability, in *Shock Waves and High Strain Rate Phenomenon in Metals*, (Edited by M. A. Meyers and L. E. Murr), pp. 277–283. Plenum Press, New York (1981).
19. T. W. Wright and J. W. Walter, On stress collapse in adiabatic shear bands. *J. Mech. Phys. Solids* **35**, 701 (1987).
20. R. C. Batra and C. H. Kim, Adiabatic shear banding in elastic-viscoplastic nonpolar and dipolar materials. *Int. J. Plasticity* **6**, 127 (1990).
21. R. C. Batra and C. H. Kim, Effect of viscoplastic flow rules on the initiation and growth of shear bands at high strain rates. *J. Mech. Phys. Solids* **38**, 859 (1990).
22. T. W. Wright and R. C. Batra, The initiation and growth of adiabatic shear bands. *Int. J. Plasticity* **1**, 205 (1985).
23. F. H. Wu and L. B. Freund, Deformation trapping due to thermoplastic instability in one-dimensional wave propagation. *J. Mech. Phys. Solids* **32**, 119 (1984).

24. C. Fressengeas, Adiabatic shear morphology at very high strain rates. *Int. J. Impact Engng* **8**, 141 (1989).
25. J. LeMonds and A. Needleman, Finite element analyses of shear localization in rate and temperature dependent solids. *Mech. Mater.* **5**, 339 (1986).
26. J. LeMonds and A. Needleman, An analysis of shear band development incorporating heat conduction. *Mech. Mater.* **5**, 363 (1986).
27. A. Needleman, Dynamic shear band development in plane strain. *ASME J. appl. Mech.* **56**, 1 (1989).
28. H. M. Zbib and E. C. Aifantis, On the localization and postlocalization behavior of plastic deformation. I. On the initiation of shear bands. *Res. Mechanica* **23**, 261 (1988).
29. L. Anand, A. M. Lush and K. H. Kim, Thermal aspects of shear localization in viscoplastic solids, in *Thermal Aspects in Manufacturing* (Edited by M. H. Attia and L. Kops), Vol. 30, pp. 89–103 ASME-PED (1988).
30. R. C. Batra and D. S. Liu, Adiabatic shear banding in plane strain problems. *ASME J. appl. Mech.* **56**, 527 (1989).
31. R. C. Batra and D. S. Liu, Adiabatic shear banding in dynamic plane strain compression of a viscoplastic material. *Int. J. Plasticity* **6**, 231 (1990).
32. Z. G. Zhu and R. C. Batra, Dynamic shear band development in plane strain compression of a viscoplastic body containing a rigid inclusion. *Acta Mech.* **84**, 89 (1990).
33. R. C. Batra and Xiang-Tong Zhang, Shear band development in dynamic loading of a viscoplastic cylinder containing two voids. *Acta Mech.* **85**, 221 (1990).
34. R. C. Batra and Z. G. Zhu, Dynamic shear band development in a thermally softening bimetallic body containing two voids. *Acta Mech.* **86**, 31 (1990).
35. L. L. Wang, H. S. Bao and W. X. Lu, The dependence of adiabatic shear bands in strain-rate, strain and temperature. *J. Physique* **49**, 207 (1988).
36. S. R. Bodner and Y. Partom, Constitutive equations for elastic-viscoplastic strain-hardening materials. *J. appl. Mech.* **42**, 385 (1975).
37. C. W. Gear, *Numerical Initial Value Problems in Ordinary Differential Equations.* Prentice-Hall, Englewood Cliffs, NJ (1971).
38. A. C. Hindmarsh, ODEPACK, a systematized collection of ODE solvers, in *Scientific Computing* (Edited by R. S. Stepleman *et al.*), pp. 55–64. North-Holland, Amsterdam (1983).
39. A. Goldsmith, T. E. Waterman and H. J. Hirschhorn, *Handbook of Thermophysical Properties of Solid Materials*, Vol. 2. MacMillan, New York (1961).
40. R. C. Batra and C. H. Kim, Effect of thermal conductivity on the initiation, growth and band width of adiabatic shear bands. *Int. J. Engng Sci.* **29**, 949 (1991).